

PAPER • OPEN ACCESS

A New 4-D Multistable Hyperchaotic Two-Scroll System, its Bifurcation Analysis, Synchronization and Circuit Simulation

To cite this article: Sundarapandian Vaidyanathan *et al* 2021 *J. Phys.: Conf. Ser.* **1764** 012206

View the [article online](#) for updates and enhancements.

You may also like

- [Synchronization and anti-synchronization of a new hyperchaotic Lü system with uncertain parameters via the passive control technique](#)
Xiaobing Zhou, Bing Kong and Haiyan Ding
- [Dynamic analysis of a fractional-order hyperchaotic system and its application in image encryption](#)
Qianqian Shi, Xinlei An, Li Xiong et al.
- [A new hyperchaotic complex system and its synchronization realization](#)
Zhengfeng Li, Fangfang Zhang, Xue Zhang et al.



The Electrochemical Society
Advancing solid state & electrochemical science & technology

243rd ECS Meeting with SOFC-XVIII

More than 50 symposia are available!

Present your research and accelerate science

Boston, MA • May 28 – June 2, 2023

[Learn more and submit!](#)

A New 4-D Multistable Hyperchaotic Two-Scroll System, its Bifurcation Analysis, Synchronization and Circuit Simulation

Sundarapandian Vaidyanathan^{1*}, Aceng Sambas², Mujiarto², Mustafa Mamat³, Wilarso⁴, Mada Sanjaya W.S.⁵, Akhmad Sutoni⁶ and I Gunawan⁷

¹Research and Development Centre, Vel Tech University, Avadi, Chennai, India

²Department of Mechanical Engineering, Universitas Muhammadiyah Tasikmalaya, Indonesia

³Faculty of Informatics and Computing, Universiti Sultan Zainal Abidin, Kuala Terengganu, Malaysia

⁴Department of Mechanical Engineering, Sekolah Tinggi Teknologi Cileungsi, Indonesia

⁵Department of Physics, Universitas Islam Negeri Sunan Gunung Djati, Bandung, Indonesia

⁶Department of Industrial Engineering, Universitas Suryakencana, Cianjur, Indonesia

⁷Universitas Langlangbuana, Bandung, Indonesia

*sundarvtu@gmail.com

Abstract. A new 4-D hyperchaotic two-scroll system with three quadratic nonlinearities and a cubic nonlinearity is proposed in this paper. The dynamical properties of the new hyperchaotic system are described in terms of phase portraits, Lyapunov exponents, Kaplan-Yorke dimension, symmetry, dissipativity, etc. We also establish that the new hyperchaotic system has multistability with coexisting attractors. As a control application, we use integral sliding mode control for active self-synchronization of the new hyperchaotic systems as master-slave systems. As an engineering application, an electronic circuit design of the new hyperchaotic two-scroll system is developed in MultiSIM, which confirms the feasibility of the system.

Keywords: Chaos, hyperchaos, hyperchaotic systems, sliding mode control, synchronization, etc.

1. Introduction

Chaos theory deals with nonlinear dynamical systems exhibiting high sensitivity to small changes in initial conditions [1-2]. Mathematically, chaotic systems are characterized by the presence of at least one positive Lyapunov exponent. Chaotic systems have applications in several engineering areas such as chemical reactors [3-4], neuron systems [5-6], mechanical systems [7-8], circuits [9-11], oscillators [12-13], neural networks [14-15], etc.

Hyperchaotic systems are defined as chaotic systems having two or more positive Lyapunov exponents. The trajectories of hyperchaotic systems can expand in two different directions corresponding to the two positive Lyapunov exponents. Hyperchaotic systems have important engineering applications such as cryptosystems [16-17], secure communication systems [18-19], etc.

In this work, we report a new 4-D hyperchaotic two-scroll system with three quadratic nonlinearities and a cubic nonlinearity. The dynamical properties of the new hyperchaotic system are described in terms of MATLAB phase portraits, Lyapunov exponents, Kaplan-Yorke dimension,



symmetry, dissipativity, etc. We show that the new hyperchaotic system has three unstable rest points. Thus, the new system has self-excited two-scroll attractor.

Multistability is an important property of chaotic dynamical systems which is the coexistence of attractors for same parameter set but different initial conditions. In this work, it is also established that the new hyperchaotic system has multistability with coexisting attractors.

Control and synchronization of chaotic and hyperchaotic systems are important research topics in the chaos literature [20-21]. As a control application, we use integral sliding mode control for active self-synchronization of the new hyperchaotic system. Sliding mode control has attractive properties such as finite-time convergence, robust to parameter variations, etc. [22-23].

In Section 2, we describe the modelling of the new hyperchaotic two-scroll system. In Section 3, we describe a dynamic analysis of the new hyperchaotic system. In Section 4, we detail active self-synchronization design for the new hyperchaotic systems as master-slave systems via integral sliding mode control. In Section 5, we detail the circuit simulation of the new hyperchaotic system using Multisim. Finally, in Section 6, we conclude this work with a summary of main results.

2. A New Hyperchaotic Two-Scroll system with Three Nonlinearities

In this research paper, we propose a novel 4-D hyperchaotic system modelled by the dynamics

$$\begin{cases} \dot{x}_1 = a(x_2 - x_1) + bx_2x_3 + x_4 \\ \dot{x}_2 = cx_2 - x_1x_3^2 - x_4 \\ \dot{x}_3 = -4x_3 + px_1^2 + x_1x_2 \\ \dot{x}_4 = x_1 + dx_4 \end{cases} \quad (1)$$

In (1), $X = (x_1, x_2, x_3, x_4)$ is the state and a, b, c, d, p are constant parameters. We note that the 4-D system (1) has three quadratic nonlinearities and a cubic nonlinearity in the dynamics.

We shall show that the system (1) exhibits a *hyperchaotic* attractor for the parameter values

$$a = 35, b = 15, c = 20, d = 0.2, p = 0.1 \quad (2)$$

For numerical simulations, we take the initial values of the system (1) as

$$x_1(0) = 0.3, x_2(0) = 0.3, x_3(0) = 0.3, x_4(0) = 0.3 \quad (3)$$

Using Wolf algorithm [24], we calculate the Lyapunov exponents for the system (1) for the parameter values (2) and the initial values (3) for $T = 1E5$ seconds as follows:

$$LE_1 = 3.5711, LE_2 = 0.2231, LE_3 = 0, LE_4 = -22.5347 \quad (4)$$

The 4-D system (1) is hyperchaotic since it possesses two positive Lyapunov exponents as indicated in Eq. (4). Also, the sum of the Lyapunov exponents of the system (1) is negative. This establishes that the system (1) is also dissipative. Thus, we conclude from the LE spectrum (4) that the system (1) is a dissipative hyperchaotic system.

Figure 1 shows the Lyapunov exponents spectrum of the new 4-D system (1).

Figure 2 depicts the two-dimensional phase plots of the new hyperchaotic system (1) for $(a, b, c, d, p) = (35, 15, 20, 0.2, 0.1)$ and $X(0) = (0.3, 0.3, 0.3, 0.3)$.

From Figure 2, it is clear that the new hyperchaotic system (1) displays a double-scroll strange attractor.

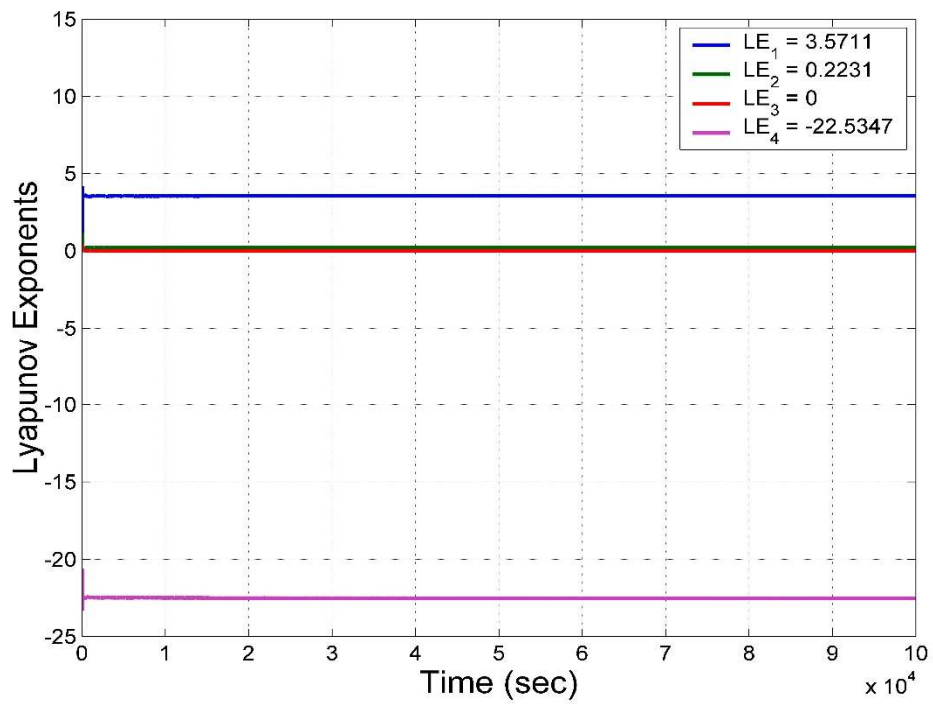


Figure 1. Lyapunov exponents of the hyperchaotic two-scroll system (1) for the parameter set $(a, b, c, d, p) = (35, 15, 20, 0.2, 0.1)$ and initial state $X(0) = (0.3, 0.3, 0.3, 0.3)$

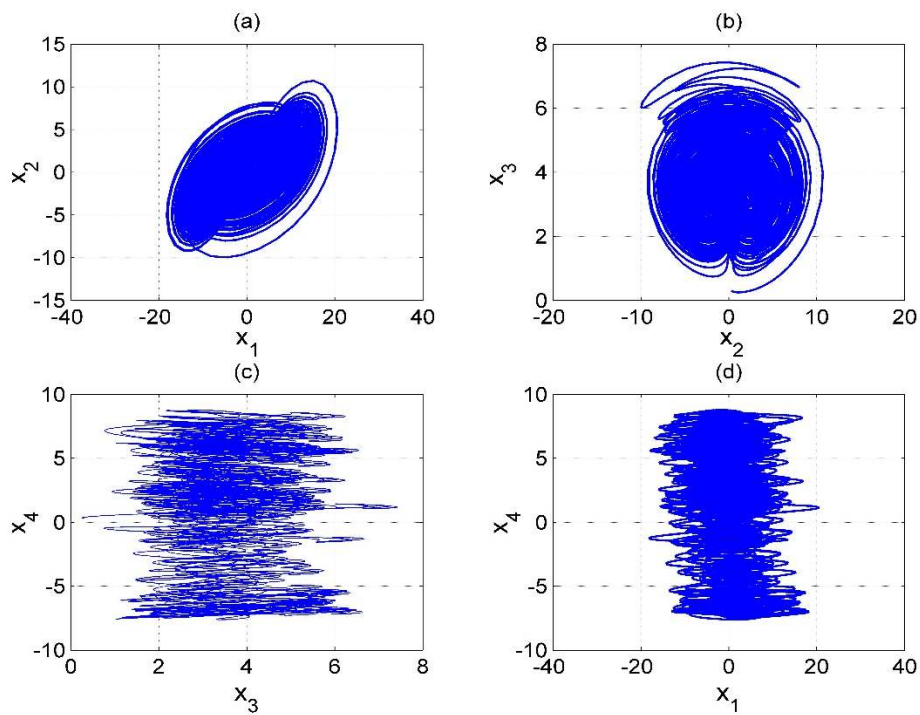


Figure 2. MATLAB 2-D plots of the new hyperchaotic two-scroll system (1) for $(a, b, c, d, p) = (35, 15, 20, 0.2, 0.1)$ and $X(0) = (0.3, 0.3, 0.3, 0.3)$

3. Dynamic Analysis of the New Hyperchaotic Two-Scroll System

3.1 Symmetry

The 4-D hyperchaotic two-scroll system (1) stays invariant under the coordinates transformation

$$(x_1, x_2, x_3, x_4) \mapsto (-x_1, -x_2, x_3, -x_4) \tag{5}$$

The invariance under the coordinates transformation (5) persists for all values of the parameters. Thus, we make the deduction that the system (1) has rotation symmetry about the $x_3 -$ axis and that any non-trivial trajectory must have a twin trajectory.

3.2 Rest Points

The rest points of the hyperchaotic system (1) are obtained by solving the following equations;

$$a(x_2 - x_1) + bx_2x_3 + x_4 = 0 \tag{6a}$$

$$cx_2 - x_1x_3^2 - x_4 = 0 \tag{6b}$$

$$-4x_3 + px_1^2 + x_1x_2 = 0 \tag{6c}$$

$$x_1 + dx_4 = 0 \tag{6d}$$

We take the parameter values as in the hyperchaotic case (2), viz.

$$a = 35, b = 15, c = 20, d = 0.2, p = 0.1 \tag{7}$$

Solving the equations (6) using the parameter values (7), we obtain three rest points:

$$E_0 = \begin{bmatrix} 0 \\ 0 \\ 0 \\ 0 \end{bmatrix}, E_1 = \begin{bmatrix} -5.2435 \\ -2.3111 \\ 3.7169 \\ 26.2173 \end{bmatrix}, E_2 = \begin{bmatrix} 5.2435 \\ 2.3111 \\ 3.7169 \\ -26.2173 \end{bmatrix} \tag{8}$$

The Jacobian matrix of the novel hyperchaotic system (1) at any point $x \in R^4$ is obtained as

$$J(x) = \begin{bmatrix} -35 & 35 + 15x_3 & 15x_2 & 1 \\ -x_3^2 & 20 & -2x_1x_3 & -1 \\ x_2 + 0.2x_1 & x_1 & -4 & 0 \\ 1 & 0 & 0 & 0.2 \end{bmatrix} \tag{9}$$

The eigenvalues of $J_0 = J(E_0)$ are numerically obtained as

$$\lambda_1 = -4, \lambda_2 = -35.0464, \lambda_3 = 0.2787, \lambda_4 = 19.9678 \tag{10}$$

This shows that E_0 is a saddle-point and hence it is unstable.

The eigenvalues of $J_1 = J(E_1)$ are numerically obtained as

$$\lambda_1 = -27.7514, \lambda_2 = 0.1832, \lambda_{3,4} = 4.3841 \pm 30.4055 i \tag{11}$$

This shows that E_1 is a saddle-focus and hence it is unstable.

The eigenvalues of $J_2 = J(E_2)$ are the same as the eigenvalues of J_1 . This shows that E_2 is a saddle-focus and hence it is unstable.

Hence, all three rest points E_0, E_1, E_2 are unstable. This shows that the hyperchaotic system (1) has a self-excited attractor [2].

3.3 Kaplan-Yorke Dimension

In Section 2, we calculated the Lyapunov exponents of the new hyperchaotic system (1) for $(a, b, c, d, p) = (35, 15, 20, 0.2, 0.1)$ and $X(0) = (0.3, 0.3, 0.3, 0.3)$ as follows:

$$LE_1 = 3.5711, LE_2 = 0.2231, LE_3 = 0, LE_4 = -22.5347 \tag{12}$$

Thus, we calculate the Kaplan-Yorke dimension of the 4-D hyperchaotic system (1) as follows:

$$D_{KY} = 3 + \frac{LE_1 + LE_2 + LE_3}{|LE_4|} = 3.1684 \tag{13}$$

The high value of D_{KY} indicates the high complexity of the new hyperchaotic system (1). Thus, the new system can be applied in many engineering applications.

3.4 Multistability

Multi-stability is a special property of a chaotic or hyperchaotic system which means the existence of coexisting attractors for the same set of parameter values but different initial states.

Figure 3 shows the multi-stability of the new hyperchaotic system (1) with two coexisting hyperchaotic attractors for $(a, b, c, d, p) = (35, 15, 20, 0.2, 0.1)$ and the initial states $X_0 = (0.3, 0.3, 0.3, 0.3)$ (blue trajectory) and $Y_0 = (-0.6, -0.6, 0.4, 0.4)$ (red trajectory).

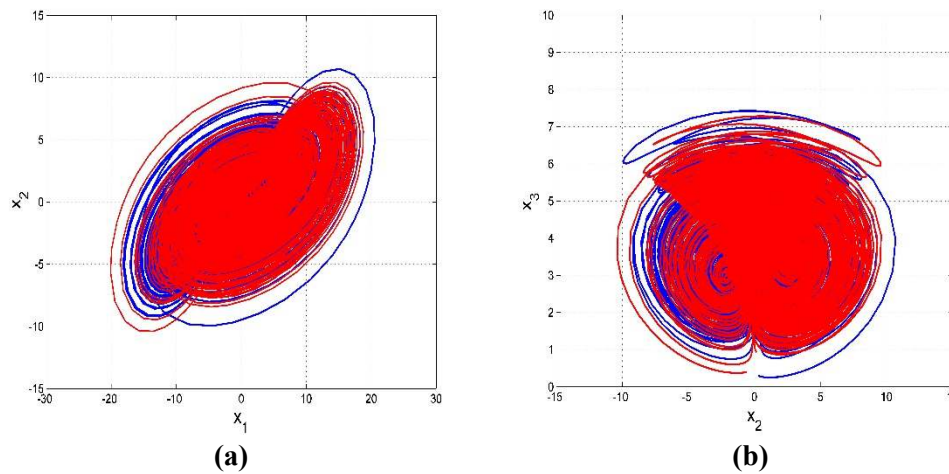


Figure 3. Multi-stability of the new hyperchaotic two-scroll system (1) with coexisting attractors for $(a, b, c, d, p) = (35, 15, 20, 0.2, 0.1)$ and the initial states $X_0 = (0.3, 0.3, 0.3, 0.3)$ (blue trajectory) and $Y_0 = (-0.6, -0.6, 0.4, 0.4)$ (red trajectory)

4. Active Synchronization of the New Hyperchaotic Systems via Integral Sliding Mode Control

In this section, we apply integral sliding mode control to achieve complete synchronization of the new hyperchaotic systems taken as master and slave systems via integral sliding mode control.

The main control result of this section is established using Lyapunov stability theory [25].

As the master system, we consider the new hyperchaotic system given by

$$\begin{cases} \dot{x}_1 = a(x_2 - x_1) + bx_2x_3 + x_4 \\ \dot{x}_2 = cx_2 - x_1x_3^2 - x_4 \\ \dot{x}_3 = -4x_3 + px_1^2 + x_1x_2 \\ \dot{x}_4 = x_1 + dx_4 \end{cases} \tag{14}$$

In (14), $X = (x_1, x_2, x_3, x_4)$ is the state and a, b, c, d are positive parameters.

As the slave system, we take the new hyperchaotic system given by

$$\begin{cases} \dot{y}_1 = a(y_2 - y_1) + by_2y_3 + y_4 + u_1 \\ \dot{y}_2 = cy_2 - y_1y_3^2 - y_4 + u_2 \\ \dot{y}_3 = -4y_3 + py_1^2 + y_1y_2 + u_3 \\ \dot{y}_4 = y_1 + dy_4 + u_4 \end{cases} \quad (15)$$

In (15), $Y = (y_1, y_2, y_3, y_4)$ is the state and u_1, u_2, u_3, u_4 are sliding mode controls.

We use integral sliding mode control to achieve global hyperchaos synchronization between (14) and (15) for all values of the initial states of the two systems and all values of the system parameters.

We define the complete synchronization error as

$$\begin{cases} e_1 = y_1 - x_1 \\ e_2 = y_2 - x_2 \\ e_3 = y_3 - x_3 \\ e_4 = y_4 - x_4 \end{cases} \quad (16)$$

The error dynamics is calculated as follows:

$$\begin{cases} \dot{e}_1 = a(e_2 - e_1) + e_4 + b(y_2y_3 - x_2x_3) + u_1 \\ \dot{e}_2 = ce_2 - e_4 - y_1y_3^2 + x_1x_3^2 + u_2 \\ \dot{e}_3 = -4e_3 + p(y_1^2 - x_1^2) + y_1y_2 - x_1x_2 + u_3 \\ \dot{e}_4 = e_1 + de_4 + u_4 \end{cases} \quad (17)$$

For each error variable, the integral sliding manifold is defined as follows:

$$\begin{cases} s_1 = e_1 + \lambda_1 \int_0^t e_1(\theta) d\theta \\ s_2 = e_2 + \lambda_2 \int_0^t e_2(\theta) d\theta \\ s_3 = e_3 + \lambda_3 \int_0^t e_3(\theta) d\theta \\ s_4 = e_4 + \lambda_4 \int_0^t e_4(\theta) d\theta \end{cases} \quad (18)$$

From (18), we deduce that

$$\begin{cases} \dot{s}_1 = \dot{e}_1 + \lambda_1 e_1 \\ \dot{s}_2 = \dot{e}_2 + \lambda_2 e_2 \\ \dot{s}_3 = \dot{e}_3 + \lambda_3 e_3 \\ \dot{s}_4 = \dot{e}_4 + \lambda_4 e_4 \end{cases} \quad (19)$$

The Hurwitz condition will be satisfied if we assume that $\lambda_i > 0$ for $i = 1, 2, 3, 4$.

Based on the exponential reaching law, we set

$$\begin{cases} \dot{s}_1 = -\eta_1 \operatorname{sgn}(s_1) - k_1 s_1 \\ \dot{s}_2 = -\eta_2 \operatorname{sgn}(s_2) - k_2 s_2 \\ \dot{s}_3 = -\eta_3 \operatorname{sgn}(s_3) - k_3 s_3 \\ \dot{s}_4 = -\eta_4 \operatorname{sgn}(s_4) - k_4 s_4 \end{cases} \quad (20)$$

Comparing the equations (19) and (20), we obtain

$$\begin{cases} \dot{e}_1 + \lambda_1 e_1 = -\eta_1 \operatorname{sgn}(s_1) - k_1 s_1 \\ \dot{e}_2 + \lambda_2 e_2 = -\eta_2 \operatorname{sgn}(s_2) - k_2 s_2 \\ \dot{e}_3 + \lambda_3 e_3 = -\eta_3 \operatorname{sgn}(s_3) - k_3 s_3 \\ \dot{e}_4 + \lambda_4 e_4 = -\eta_4 \operatorname{sgn}(s_4) - k_4 s_4 \end{cases} \quad (21)$$

The equation (21) can be expanded using (17) as follows:

$$\begin{cases} a(e_2 - e_1) + e_4 + b(y_2 y_3 - x_2 x_3) + u_1 + \lambda_1 e_1 = -\eta_1 \operatorname{sgn}(s_1) - k_1 s_1 \\ ce_2 - e_4 - y_1 y_3^2 + x_1 x_3^2 + u_2 + \lambda_2 e_2 = -\eta_2 \operatorname{sgn}(s_2) - k_2 s_2 \\ -4e_3 + p(y_1^2 - x_1^2) + y_1 y_2 - x_1 x_2 + u_3 + \lambda_3 e_3 = -\eta_3 \operatorname{sgn}(s_3) - k_3 s_3 \\ e_1 + de_4 + u_4 + \lambda_4 e_4 = -\eta_4 \operatorname{sgn}(s_4) - k_4 s_4 \end{cases} \quad (22)$$

From Eq. (22), we obtain the required sliding mode control law as follows:

$$\begin{cases} u_1 = -a(e_2 - e_1) - e_4 - b(y_2 y_3 - x_2 x_3) - \lambda_1 e_1 - \eta_1 \operatorname{sgn}(s_1) - k_1 s_1 \\ u_2 = -ce_2 + e_4 + y_1 y_3^2 - x_1 x_3^2 - \lambda_2 e_2 - \eta_2 \operatorname{sgn}(s_2) - k_2 s_2 \\ u_3 = 4e_3 - p(y_1^2 - x_1^2) - y_1 y_2 + x_1 x_2 - \lambda_3 e_3 - \eta_3 \operatorname{sgn}(s_3) - k_3 s_3 \\ u_4 = -e_1 - de_4 - \lambda_4 e_4 - \eta_4 \operatorname{sgn}(s_4) - k_4 s_4 \end{cases} \quad (23)$$

Theorem 1. The new hyperchaotic two-scroll systems (14) and (15) are globally and asymptotically synchronized for all initial conditions by the integral sliding mode controller (23), where the constants λ_i, η_i, k_i , ($i = 1, 2, 3, 4$) are all positive.

Proof. We establish this theorem using Lyapunov stability theory [25].

First, we consider the quadratic Lyapunov function given by

$$V(s_1, s_2, s_3, s_4) = \frac{1}{2} (s_1^2 + s_2^2 + s_3^2 + s_4^2) \quad (24)$$

Clearly, V is positive definite at all points of R^4 . The time-derivative of V is obtained as

$$\dot{V} = \sum_{i=1}^4 s_i [-\eta_i \operatorname{sgn}(s_i) - k_i s_i] = \sum_{i=1}^4 [-\eta_i |s_i| - k_i s_i^2] \quad (25)$$

From (25), we see that \dot{V} is negative definite at all points of R^4 .

Using Lyapunov stability theory, we conclude that $s_i(t) \rightarrow 0$ as $t \rightarrow \infty$ for each $i = 1, 2, 3, 4$.

Hence, it follows that $e_i(t) \rightarrow 0$ as $t \rightarrow \infty$ for each $i = 1, 2, 3, 4$. This completes the proof. ■

For numerical simulations, we take the system parameters as in hyperchaotic case (2), viz. $(a, b, c, d, p) = (35, 15, 20, 0.2, 0.1)$. We take the sliding constants as $\lambda_i = \mu_i = 0.1$ and $k_i = 20$ for each $i = 1, 2, 3, 4$. We take the initial state of the hyperchaotic system (14) as $X(0) = (3.2, 5.7, 12.3, 3.9)$. We take the initial state of the hyperchaotic system (15) as $Y(0) = (7.3, 2.5, 1.8, 11.3)$. Figures 4 and 5 show the complete synchronization between the hyperchaotic systems (14) and (15).

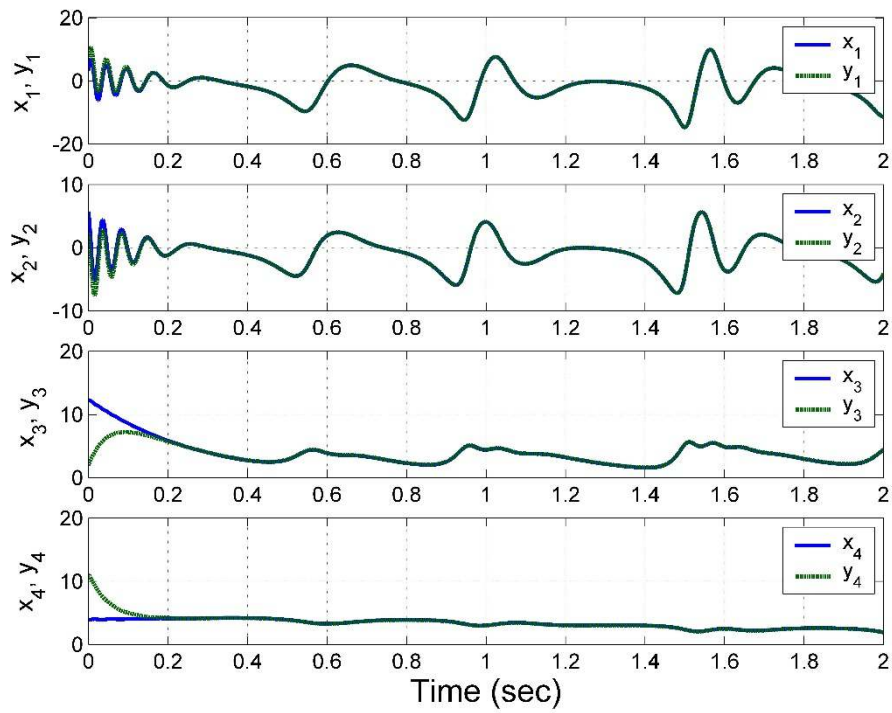


Figure 4. Complete synchronization of the hyperchaotic systems (14) and (15)

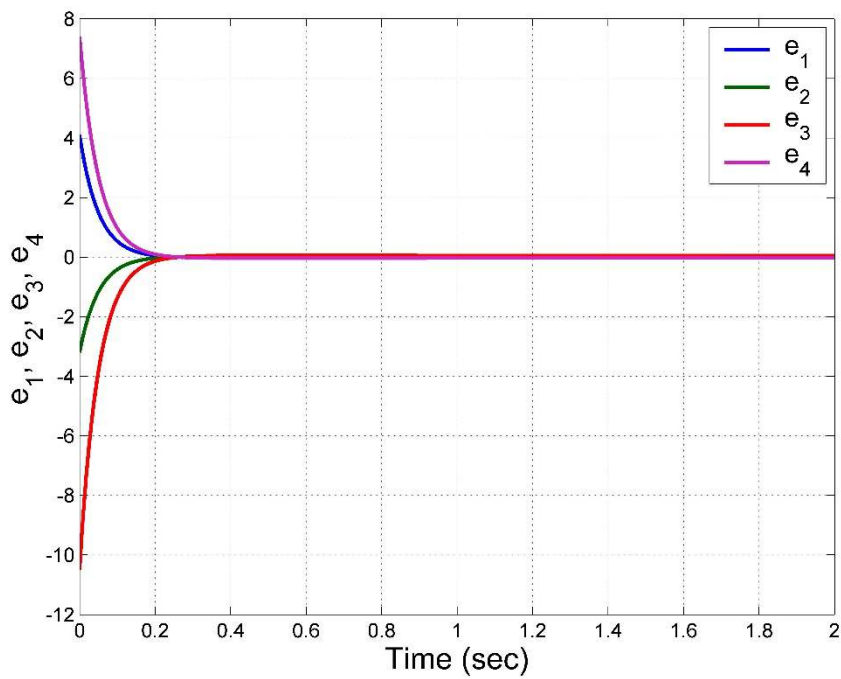


Figure 5. Time-plot of the synchronization errors between the hyperchaotic systems (14) and (15)

5. Circuit Simulation of the New Hyperchaotic System

This study will consider the analog circuit implementation of the new hyperchaotic two-scroll system described in (1). Figure 6 shows a four channels electronic circuit scheme with variables x_1, x_2, x_3, x_4 from the system (1). The dynamics of the new hyperchaotic two-scroll system is described as follows:

$$\begin{cases} \dot{x}_1 = \frac{1}{C_1 R_1} x_2 - \frac{1}{C_1 R_2} x_1 + \frac{1}{10 C_1 R_3} x_2 x_3 + \frac{1}{C_1 R_4} x_4 \\ \dot{x}_2 = \frac{1}{C_2 R_5} x_2 - \frac{1}{100 C_2 R_6} x_1 x_3^2 - \frac{1}{C_2 R_7} x_4 \\ \dot{x}_3 = -\frac{1}{C_3 R_8} x_3 + \frac{1}{10 C_3 R_9} x_1^2 + \frac{1}{10 C_3 R_{10}} x_1 x_2 \\ \dot{x}_4 = \frac{1}{C_4 R_{11}} x_1 + \frac{1}{C_4 R_{12}} x_4 \end{cases} \quad (26)$$

Here, x_1, x_2, x_3, x_4 are the voltages across the capacitors C_1, C_2, C_3 and C_4 , respectively. We choose the values of the circuit elements as $R_1 = R_2 = 11.42 \text{ k}\Omega$, $R_3 = 2.67 \text{ k}\Omega$, $R_5 = 20 \text{ k}\Omega$, $R_6 = 4 \text{ k}\Omega$, $R_{10} = 40 \text{ k}\Omega$, $R_{12} = 2 \text{ M}\Omega$, $R_4 = R_7 = R_9 = R_{11} = 400 \text{ k}\Omega$, $R_8 = R_{13} = R_{14} = R_{15} = R_{16} = R_{17} = R_{18} = 100 \text{ k}\Omega$, $C_1 = C_2 = C_3 = C_4 = 3.2 \text{ nF}$. The corresponding phase portraits on the oscilloscope are shown in Figure 7. The agreement between the Multisim results (Figure 7) and the MATLAB plots (Figure 2).

6. Conclusions

In this work, we described a new four-dimensional hyperchaotic two-scroll system with four nonlinearities (three quadratic nonlinearities and a cubic nonlinearity). We detailed the qualitative and dynamical properties of the new hyperchaotic two-scroll system in terms of phase portraits, Lyapunov exponents, Kaplan-Yorke dimension, symmetry, dissipativity, rest points, etc. We also established that the new hyperchaotic two-scroll system has multistability with coexisting attractors. As a control application, we applied integral sliding mode control to achieve active self-synchronization of the new hyperchaotic system. As an engineering application, an electronic circuit realization of the new hyperchaotic two-scroll system was developed in Multisim and confirmed the feasibility of the system. The circuit design in Multisim of the new hyperchaotic two-scroll system enable numerous applications of the new hyperchaotic two-scroll system in areas such as encryption and secure communication.

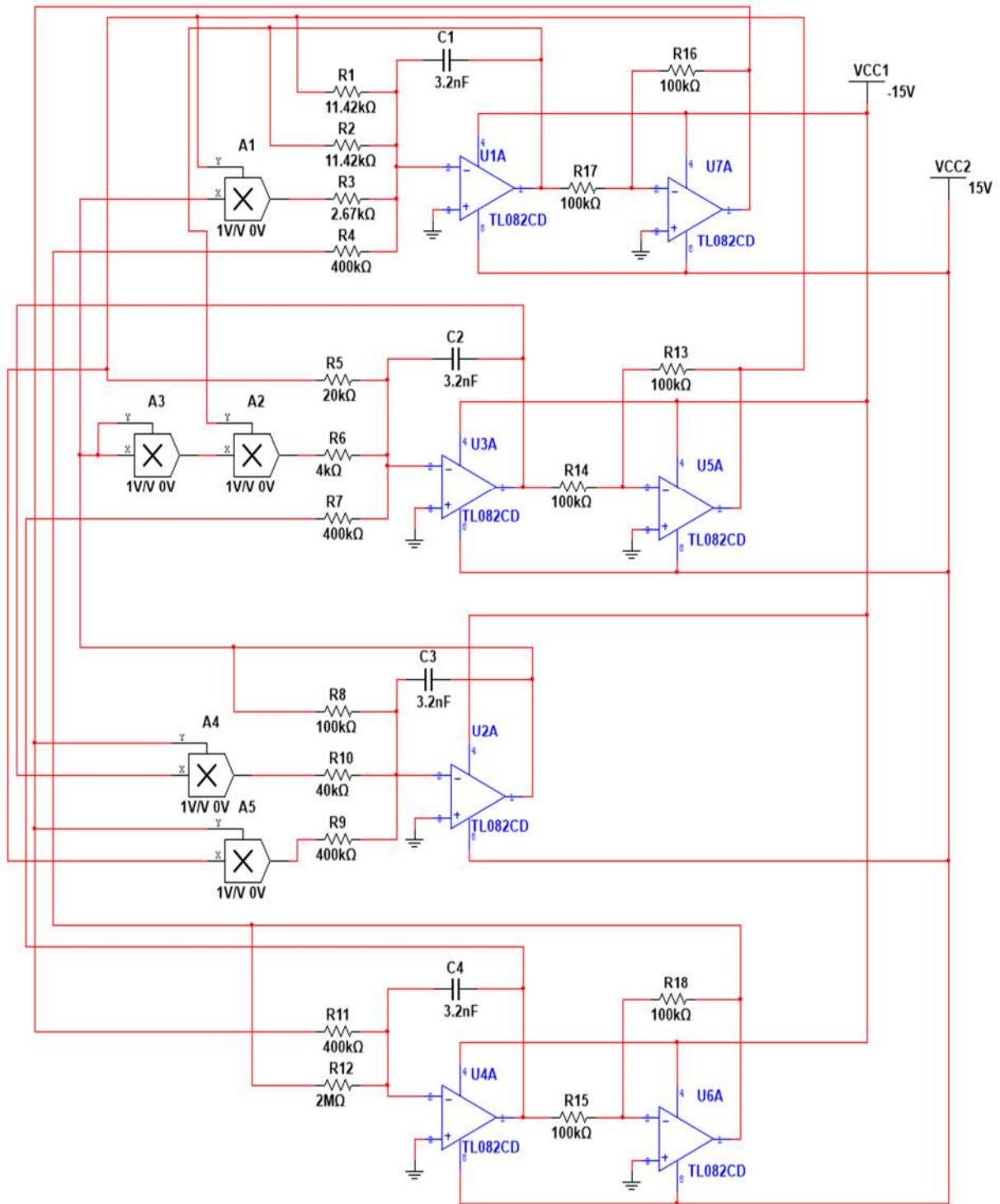


Figure 6. Circuit design for the new hyperchaotic two-scroll system

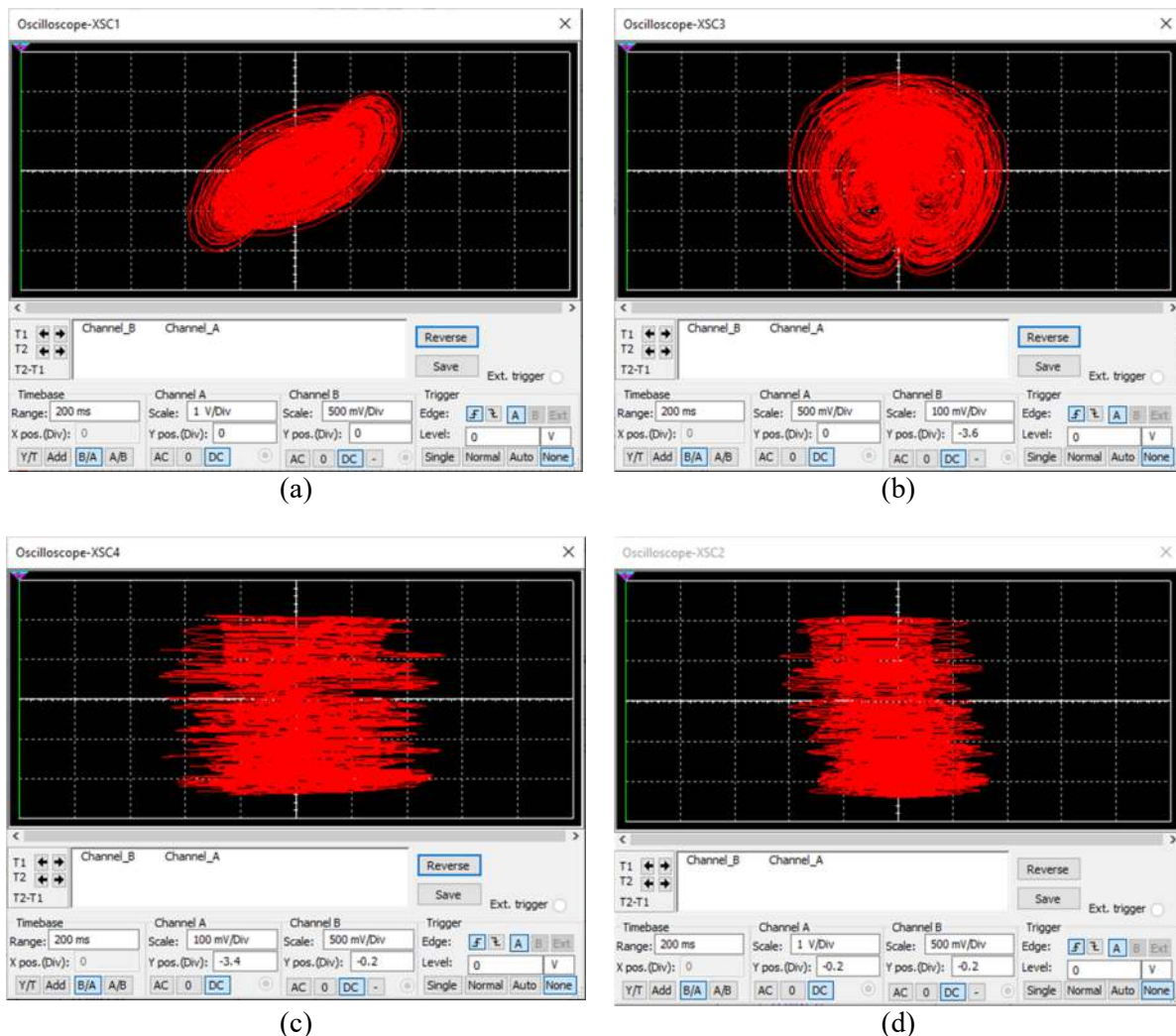


Figure 7. MultiSIM chaotic attractors of the new hyperchaotic two-scroll system (a) $x_1 - x_2$ plane, (b) $x_2 - x_3$ plane, (c) $x_3 - x_4$ plane and (d) $x_1 - x_4$ plane.

References

- [1] Vaidyanathan S and Volos C 2017 *Advances and Applications in Chaotic Systems* (Berlin: Springer)
- [2] Pham V T, Vaidyanathan S, Volos C and Kapitaniak T 2018 *Nonlinear Dynamical Systems with Self-Excited and Hidden Attractors* (Berlin: Springer)
- [3] Muzzio F J and Liu M 1996 *The Chemical Engineering Journal and the Biochemical Engineering Journal* **64** 117-127
- [4] Awal N M and Epstein I R 2020 *Physical Review E* **101** 042222
- [5] Luo H and Ma J 2020 *International Journal of Modern Physics B* **34** 2050137
- [6] He Z, Li C, Chen L and Cao Z 2020 *Neural Networks* **121** 497-511
- [7] Sundarapandian V 2013 *Lecture Notes in Electrical Engineering* **131** 319-327
- [8] Belato D, Weber H I, Balthazar J M and Mook D T 2001 *International Journal of Solids and Structures* **38** 1699-1706
- [9] Liu C X, Yan Y and Wang W Q 2020 *Applied Mathematical Modelling* **79** 469-489

- [10] Sambas A, Vaidyanathan S, Zhang S, Zeng Y, Mohamed M A and Mamat M 2019 *IEEE Access* **7** 115454-115462
- [11] Sambas A, Vaidyanathan S, Tlelo-Cuautle E, Zhang S, Guillen-Fernandez O, Sukono, Hidayat Y and Gundara G 2019 *Electronics* **8** 1211
- [12] Tamaševičius A, Mykolaitis G, Bumelienė S, Baziliauskas A, Krivickas R and Lindberg E 2006 *Nonlinear Dynamics* **44** 159-165
- [13] Vaidyanathan S 2015 *Kyungpook Mathematical Journal* **55** 563-586
- [14] Lin H, Wang C and Tan Y 2020 *Nonlinear Dynamics* **99** 2369-2386
- [15] Fei Z, Guan C and Gao H 2017 *IEEE transactions on neural networks and learning systems* **29** 2558-2567
- [16] Grassi G and Mascolo S 1999 *IEEE Transactions on Circuits and Systems I: Fundamental Theory and Applications* **46** 1135-1138
- [17] Jeng F G, Huang W L and Chen T H 2015 *Signal Processing: Image Communication*, **34** 45-51.
- [18] Roy A, Misra A P and Banerjee S 2019 *Optik* **176** 119-131
- [19] Wang J, Yu W, Wang J, Zhao Y, Zhang J and Jiang D 2019 *International Journal of Circuit Theory and Applications* **47** 702-717
- [20] Rabah K and Ladaci S 2020 *Circuits, Systems and Signal Processing* **39** 1244-1264
- [21] Medhaffar H, Feki M and Derbel N 2020 *International Journal of Automation and Control* **14** 115-137
- [22] Ren J, He G and Fu J 2020 *Information Sciences* **535** 42-63
- [23] Halder A, Pal N and Mondal D 2020 *Mathematics and Computers in Simulation* **177** 244-262
- [24] Wolf A, Swift J B, Swinney H L and Vastano J A 1985 *Physica D* **16** 285-317
- [25] Khalil H K 2001 *Nonlinear Systems* (New York: Pearson)